ACS MEASUREMENT SCIENCE Au
AN OPEN ACCESS JOURNAL OF THE AMERICAN CHEMICAL SOCIETY

pubs.acs.org/measureau

Article

Leukocyte Depletion and Size-Based Enrichment of Circulating Tumor Cells Using a Pressure-Sensing Microfiltration Device

Daisuke Onoshima,* Tetsunari Hase,* Naoto Kihara, Daiki Kuboyama, Hiromasa Tanaka, Naoya Ozawa, Hiroshi Yukawa, Mitsuo Sato, Kenji Ishikawa, Yoshinori Hasegawa, Makoto Ishii, Masaru Hori, and Yoshinobu Baba

Cite This: *ACS Meas. Sci. Au* 2023, 3, 113–119

Read Online

ACCESS | Metrics & More | Article Recommendations | Supporting Information

ABSTRACT: Considering the challenges in isolating circulating tumor cells (CTCs) pertaining to cellular stress and purity, we report the application of a blood microfiltration device as an optimal approach for noninvasive liquid biopsy to target CTCs. We experimentally analyzed the filtration behavior of the microfilter using pressure sensing to separate tumor cells from leukocytes in whole blood. This approach achieved an average recovery of >96% of the spiked tumor cells and depletion of >99% of total leukocytes. Furthermore, we carried out genomic profiling of the CTCs using the blood microfiltration device. The method was also applied in a clinical setting; DNA amplification was performed using a small number of microfiltered CTCs and epidermal growth factor receptor mutations were successfully detected to characterize the efficacy of molecularly targeted drugs against lung cancer. Overall, the proposed method can provide a tool for evaluating efficient filtration pressure to concentrate CTCs from whole blood.

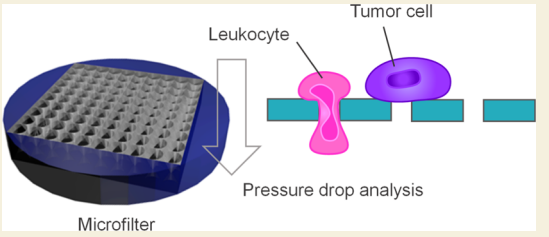

KEYWORDS: *microfiltration, circulating tumor cells, pressure sensing, epidermal growth factor receptor, lung cancer*

INTRODUCTION

Rapid and highly efficient isolation of circulating tumor cells (CTCs) from peripheral blood is useful for noninvasive cancer detection and subtyping via liquid biopsy.[1,2] For example, genomic profiling of CTCs provides useful information for analyzing the evolution of major genotypes associated with treatment response or disease progression.[3] Information on these mutations can be used to select molecularly targeted anticancer drugs. These drugs exert antitumor effects by inhibiting the signaling of specific molecules, including tyrosine kinases, which are involved in cancer cell growth. Epidermal growth factor receptor (EGFR) is one of the most mutated genes in non-small cell lung cancer (NSCLC); EGFR mutations result in constitutive cell growth even in the absence of growth factors.[4]

Isolation of CTCs from whole blood remains a challenge. Many reports on CTCs have highlighted technological developments for their separation.[5−7] Filtration based on cell size is one such technique that focuses on the physical characteristics of CTCs. During the physical separation process, the cells are placed under excessive stress due to shear forces, non-physiological temperatures, and additives. These stresses can cause transcriptional and epigenetic changes, such as histone modifications, which potentially result in lower separation efficiency.[8] Therefore, reducing these cellular stresses may be important in the process of isolating CTCs from whole blood.

CTC purity is an important factor for cancer gene mutation analysis using contamination-sensitive technologies, such as real-time polymerase chain reaction (PCR) and next-generation sequencing.[9] Most nucleated cells in the blood are leukocytes. In 1 mL of blood from a patient with cancer, dozens of CTCs are intermingled with approximately 1 million white blood cells.[10] Previously, our research group reported a size-exclusive microfiltration device developed for tumor cell separation.[11] The separation of CTCs by size exclusion has the advantage of being independent of cell surface markers.[12−15] However, size-based approaches are susceptible to overlaps in size and density of CTCs and leukocytes.

Herein, we demonstrated the application of our microfiltration device for size-based enrichment of tumor cells along with leukocyte depletion by measuring the filtration pressure. Pore pattern and pressure drop were analyzed as filtration parameters affecting CTC enrichment. Furthermore, we conducted a mutational analysis of CTCs in a clinical sample using single-cell DNA amplification. It demonstrates the filtration pore pattern and pressure drop for a practical level

Received: October 5, 2022
Revised: November 29, 2022
Accepted: November 30, 2022
Published: December 8, 2022

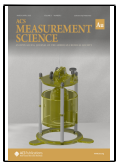

https://doi.org/10.1021/acsmeasuresciau.2c00057
ACS Meas. Sci. Au 2023, 3, 113–119

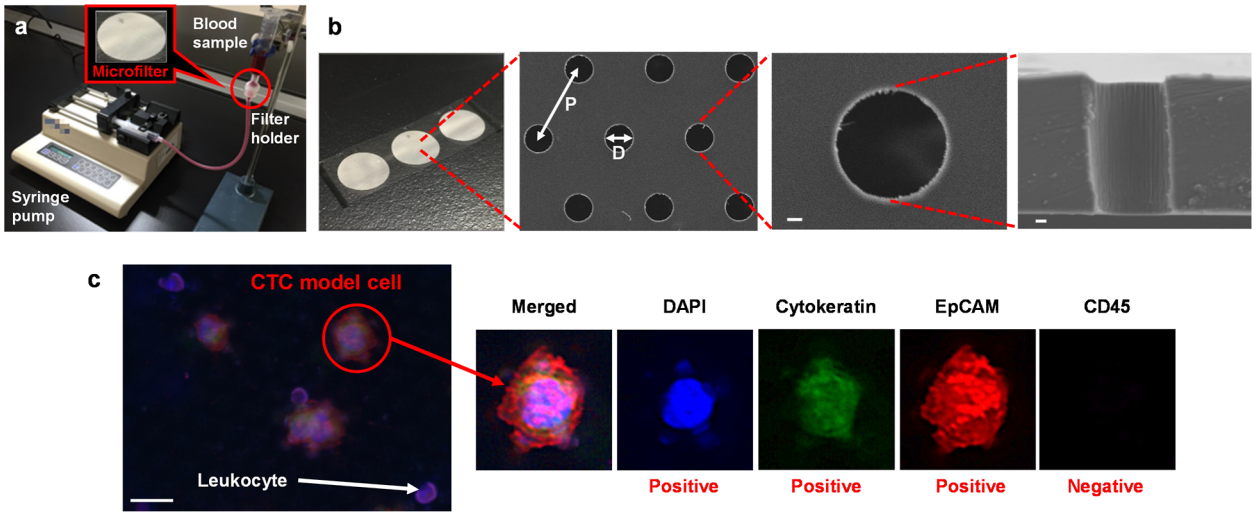

Figure 1. Blood microfiltration device for separating and staining tumor cells. (a) Photograph of the microfiltration device. (b) Photograph of a 13 mm filter and scanning electron microscopy images of the holes. *D* (hole diameter) and *P* (pitch) are defined as shown in the image. Pitch refers to the distance between two holes. Scale bars indicate 1 μm. (c) Results of multi-staining of single cells recovered from blood. The scale bar indicates 30 μm.

of enrichment that meets the genetic analysis of CTCs in membrane separation for many microfluidic analyses. This provides useful information for the design of filters for membrane separation of CTCs and other rare cells. The syringe pump was selected because it has been used in microanalysis[16] as a device to supply a constant flow rate to a filter. Syringe pumps have been used in many past CTC analyzers.[13−15,17] In this paper, all experiments were conducted using syringe pumps in consideration of the expected filter applications.

EXPERIMENTAL SECTION

Cell Culture

We cultured NSCLC cells (H358, H1975) in 2 mM L-glutamine (Thermo Fisher Scientific), 10% (v/v) FBS (Biowest), and 1% (v/v) penicillin/streptomycin solution (Thermo Fisher Scientific) at 37 °C for 3−4 days in RPMI 1640 medium containing 5% CO_2 in a humidified atmosphere. Confluent cells were trypsinized and resuspended in phosphate-buffered saline (PBS) immediately prior to each experiment. Cell diameter of H358 was measured with a handheld automated cell counter (Merck Scepter 2.0).

Microfiltration Device

We used ethylene tetrafluoroethylene (ETFE) low-autofluorescence fluoropolymer membrane filters for cell filtration. The detailed procedure for fabricating microfilters has been previously described.[11] ETFE filters were inserted into a filter holder (SWINNEX SX0001300) and on the upper side of the filter holder, and a syringe for the samples (TERUMO ss-10ESz) was placed. The syringe for the effluent was set in a syringe pump (KD Scientific KDS210) and connected to the lower side of the filter holder with a Safeed extension tube (TERUMO SF-ET1725).

Immunostaining and Microscopic Imaging of Cells

Mounting solution with DAPI dilactate and enumeration staining solution for cytokeratin, EpCAM, and CD45 (Creatv Microtech CellSieve CTC enumeration kit) were used for cell imaging. Hoechst 33342 Dojindo, Vimentin Ab128507 (FITC), CD45 Alexa Fluor 647 BioLegend, and EpCAM PE (BD Biosciences) were used for analyzing clinical samples. Antibody staining was performed on a filter for 50 min while passing 200 μL of the staining solution at 4 μL/min. Excess dye remaining on the microfilter was removed using 3 mL of PBST. A fluorescence microscope (Keyence Biorevo BZ-X710 or EVOS Cell Imaging Systems, Thermo Fisher Scientific) with appropriate fluorescence filter sets was used to acquire images of the cells.

Pressure Sensing

A blood pressure monitoring kit (DX360 NIHON KOHDEN) was combined with a bridge amplifier (ADInstruments FE221) and an AD converter (ADInstruments ML826 PowerLab 2/26) to measure the differential pressure for microfiltration. Differential pressure was calculated by detecting the pressures upstream and downstream of the filter using a transducer. The pressure drop was evaluated from the differential pressure 300 s after initiating filtration.

Real-Time PCR

Cells were collected from the microfilters using a Micro Pick and Place Z robotic system (Nepa Gene MPP-200Z). DNA extraction and amplification were performed using the REPLI-g Single Cell Kit (Qiagen 150345) or Ampli1 Whole Genome Amplification Kit (Menarini Silicon Biosystems) and a real-time PCR system (NIPPON Genetics LightCycler 96 system). A therascreen EGFR RGQ PCR Kit version 2 (Qiagen 874111) was used to detect gene mutations. The PCR consisted of 50 cycles of 30 s at 95 °C and 60 s at 60 °C.

Clinical Samples

Blood samples were obtained from a patient with pathologically diagnosed NSCLC at Nagoya University Hospital. Written informed consent was obtained from the patients. Whole blood was collected in commercially available ethylenediaminetetraacetic acid-treated tubes. We performed genetic analyses using the Cobas EGFR Mutation Test v2 (Roche Diagnostics) and a peptide nucleic acid−locked nucleic acid (PNA−LNA) PCR clamp at the laboratories of the LSI Medience Corporation (Tokyo, Japan). The Ethics Review Committee of Nagoya University Graduate School of Medicine approved this study (no. 2017-0034).

RESULTS AND DISCUSSION

Filtration Efficiency for Model CTCs and Leukocytes

Microholes of various sizes and pitches were tested using whole blood samples spiked with tumor cells and diluted twofold with PBS (Figure 1a). The microfilter was placed in a filter holder, and 7.5 mL of blood sample was aspirated at 1 mL/min. The blood samples were spiked with 1000 NSCLC cells (H358). Figure 1b shows an example of a microfilter with 380,000 microholes in a 13 mm filter format. Multiple staining

https://doi.org/10.1021/acsmeasuresciau.2c00057
ACS Meas. Sci. Au 2023, 3, 113−119

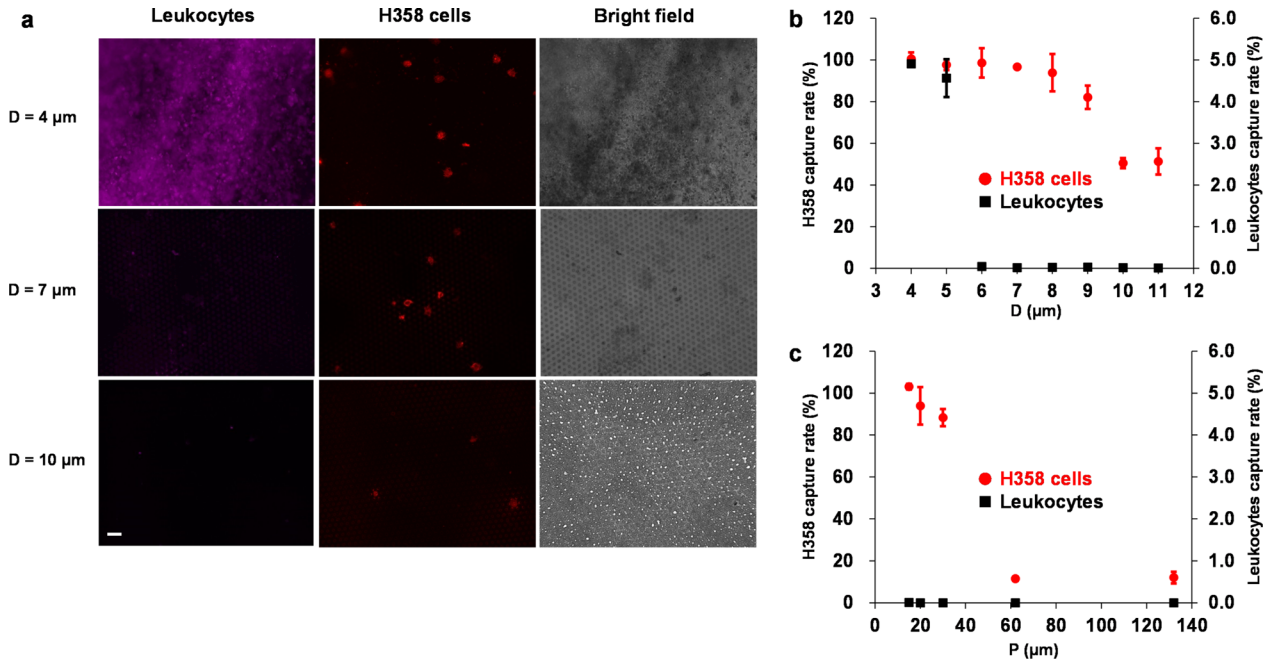

Figure 2. Analysis of filtration efficiency for tumor cells. (a) Microscopic fluorescence and bright-field images on the microfilter. The scale bar indicates 50 μm. (b) Capture rate of H358 cells and leukocytes vs hole diameter (P = 20 μm). (c) Capture rate of H358 cells and leukocytes vs pitch (D = 7 μm).

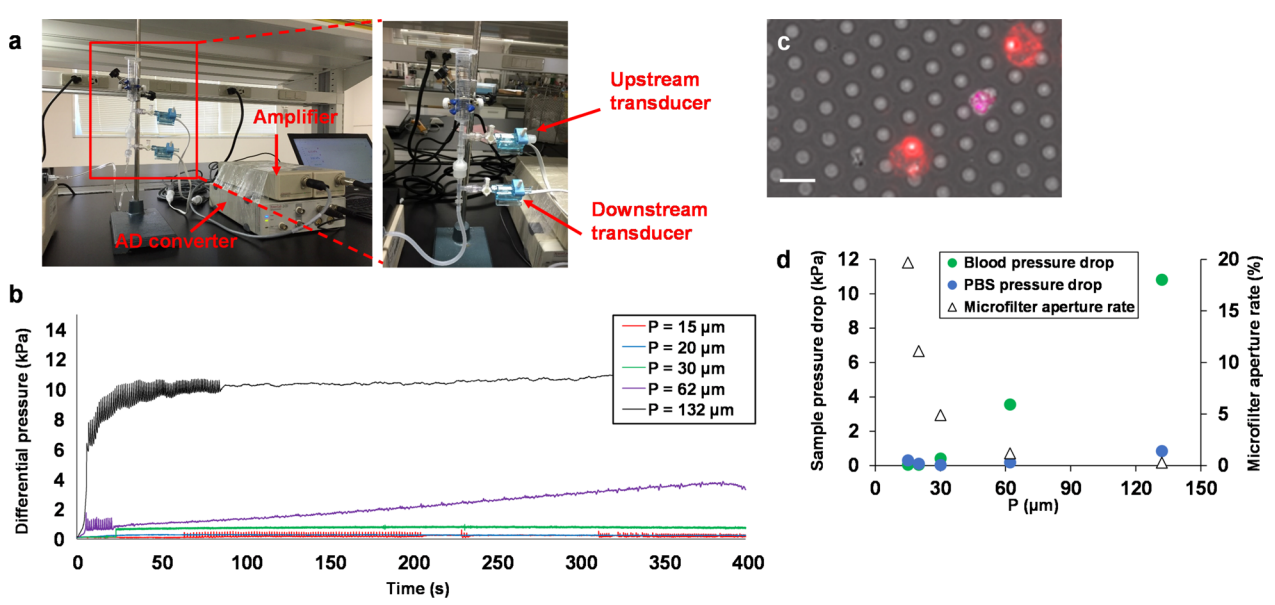

Figure 3. Measurement of differential pressure in microfiltration. (a) Photograph of the pressure sensing module. (b) Results of differential pressure monitoring using a microfilter with a 7 μm hole diameter. (c) Microscopic images of clogged H358 cells (red) and a leukocyte (pink). The scale bar indicates 20 μm. (d) Pressure drop vs aperture ratio.

with DAPI and fluorescence-tagged antibodies specific to cytokeratin (FITC), EpCAM (TRITC), and CD45 (Cy5) was performed inside the filter holder without cell fixation or permeabilization. Model CTCs with tumor markers were detected separately from leukocytes (Figure 1c). The measured cell diameter of H358 was around 16 μm. This is about 60% above the literature value for averaged leukocytes.[17]

The number of H358 cells and leukocytes captured by the microfilter varied with the hole diameter (Figure 2a,b). With hole diameters $\geq$ 10 μm, the number of H358 cells decreased markedly. Conversely, the number of leukocytes increased markedly at hole diameter $\leq$ 5 μm. When microholes with 20 μm pitch and approximately 7 μm hole diameter were used, H358 cells were captured effectively, and most leukocytes were removed. This performance corresponded to an average recovery of more than 96% of the spiked tumor cells and a reduction of more than 99% of the total leukocytes. The high capture rate of tumor cells was also verified using comparative experiments with PBS (Figure S1).

The effect of microfilter apertures on cell capture was evaluated by testing different pitches of microholes fixed at a hole diameter of 7 μm (Figure S2). The capture efficiency of H358 cells and leukocytes varied with the pitch (Figure 2c). As the pitch lengthens, the number of holes decreases and flow

https://doi.org/10.1021/acsmeasuresciau.2c00057
ACS Meas. Sci. Au 2023, 3, 113−119

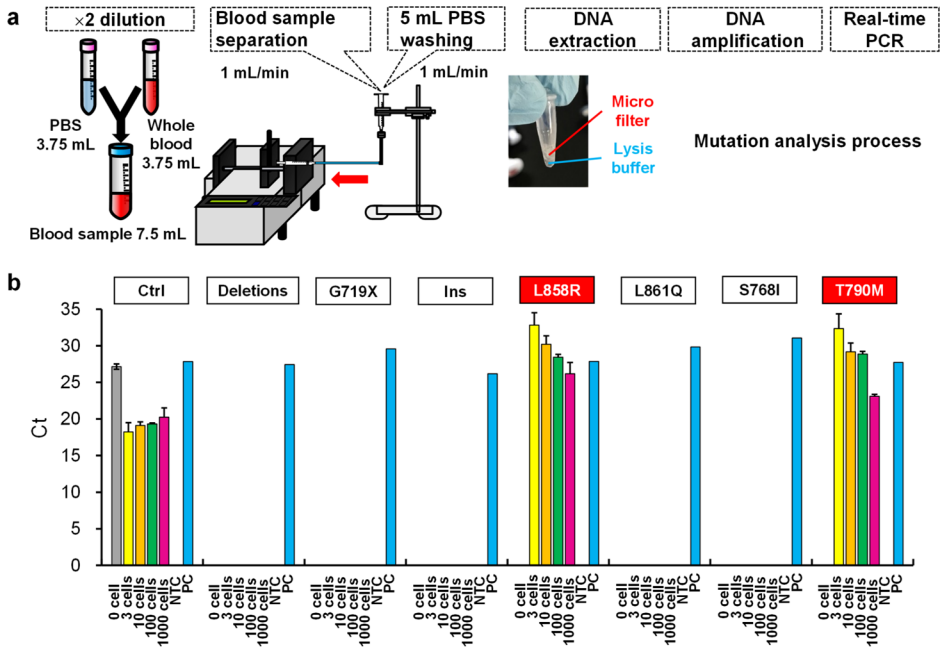

Figure 4. Analysis of DNA mutations in tumor cells. (a) Membrane isolation and real-time PCR protocol. Isolated cells were immediately immersed in lysis buffer solution and subjected to DNA extraction. (b) Quantitative PCR results for EGF receptor gene mutations in H1975 cells. 0 cell, NTC, and PC indicate the negative control (blood only), no template control (water only), and positive control, respectively. H1975 cells were isolated from blood samples using a microfilter with 20 μm pitch and 7 μm hole diameter.

resistance increases, resulting in a lower capture rate of H358 cells. When the pitch becomes shorter, the number of holes increases and the flow resistance decreases, resulting in an increase in the capture rate of H358 cells. H358 cells and leukocytes were adequately separated at a pitch of ≤30 μm. The change in pitch affects the aperture of the filter, suggesting a change in the pressure applied to capture the cells.

Pressure Drop Analysis for Microfilters with Different Pitches

Pressure measurements were taken to verify the cause of the decrease in the capture rate with decreasing number of holes, assuming a change in the pressure applied to the cells. Figure 3a shows a schematic representation of filtration pressure sensing. Pressure transducers were connected to the upstream and downstream lines of the filter holder to measure the pressure gradient across the microfilter. As shown in Figure 3b, the change in pressure during filtration was successfully monitored. The maximum pressure drop (10.82 kPa) was observed at the largest hole pitch and was caused by filter clogging of the cells.[13,17] The pressure drop mainly reflects the process of filter clogging by leukocytes.

Figure 3c shows a typical example of fluorescence microscopy and bright-field microscopy of the filter surface at increased differential pressure. Some filter holes were jammed with H358 cells and leukocytes. The differential pressure (0.42 kPa) hardly increased when the pitch was less than 30 μm. This microfilter cell separation was probably influenced by differences in cell stiffness and plasticity. For example, cancer cells are less rigid than benign cells[18] and more rigid than leukocytes.[19] The filter used in this paper is a prototype developed to analyze the filtration pore pattern and pressure drop affecting CTC enrichment. Analysis of the prototype by pressure monitoring revealed a relationship between separation performance and pressure drop.

The measured value of the blood pressure drop was plotted against the calculated value of the aperture rate at different hole pitches for the microfilter (Figure 3d). The aperture rate is the ratio of hole area to filter area. This indicator was introduced to show the change in pressure drop versus filter specification, which summarizes the relationship between pitch and number of holes. Evidence of filter clogging was apparent at aperture rates lower than 4.9%. These results reveal that pressure drops above 0.42 kPa at P = 30 μm are detrimental to the capture rate of H358 cells. No pressure drop was observed in the comparison test using PBS (Figure S3). However, a slight drop in pressure was observed in proportion to the blood dilution rate (Figure S3) and the flow rate of the syringe (Figure S4).

Quantitative PCR Analysis for EGFR Mutations

Blood samples diluted twofold in PBS were filtered and washed for subsequent mutational analysis (Figure 4a). Another NSCLC cell line, H1975, which harbors L858R and T790M mutations, was used as a model CTC line and spiked into the blood sample. The major EGFR mutations include deletions in exon 19 and an L858R substitution in exon 21, which confer sensitivity to tyrosine kinase inhibitors (TKIs), whereas T790M in exon 20 confers resistance to first- or second-generation EGFR-TKI.[20−22] A lysis buffer was used to extract DNA from cancer cells using a microfilter. Whole-genome amplification and detection of specific mutations were performed using a commercially available whole-genome amplification kit and a real-time PCR system.

Figure 4b shows the quantitative PCR results obtained from cell spiking and membrane separation tests with healthy whole blood. Blood samples were prepared by adding H1975 at 3, 10, 100, and 1000 cells. Up to 100 cells were collected and placed into blood sample tubes, and 1000 cells were estimated from serial dilutions. According to the real-time PCR Ct values, specific mutations of L858R and T790M were successfully

https://doi.org/10.1021/acsmeasuresciau.2c00057
ACS Meas. Sci. Au 2023, 3, 113−119

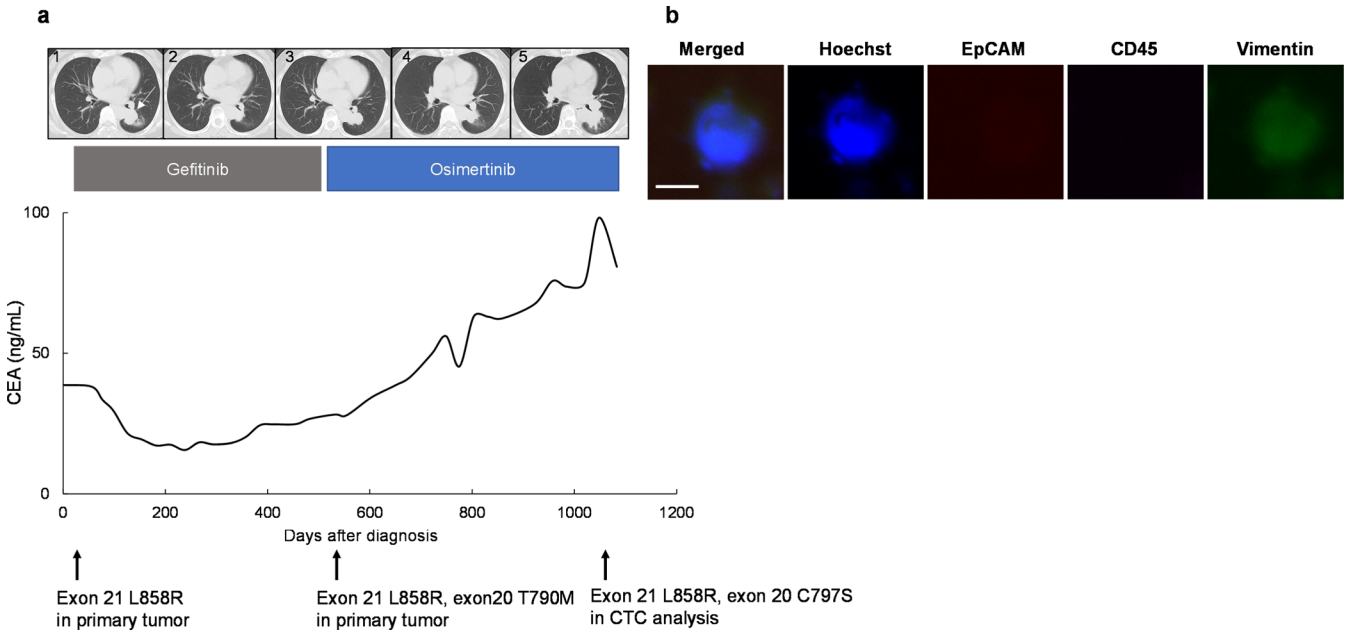

Figure 5. CTC analysis for genotyping in a patient with lung cancer. (a) Clinical course of the patient. (1) Prior to gefitinib. (2) Response to gefitinib. (3) Resistance to gefitinib. (4) Response to Osimertinib. (5) Resistance to Osimertinib. The arrow indicates the primary tumor in the left lower lobe of the lung. Mutational analyses were conducted using Cobas EGFR Mutation Test v2 or PNA−LNA PCR clamp. The CEA level was used as a tumor marker to represent the patient's tumor burden. (b) Captured CTC under a fluorescence microscope. The scale bar indicates 20 μm. CEA, carcinoembryonic antigen; CTCs, circulating tumor cells; EGFR, epidermal growth factor receptor; LNA, locked nucleic acid; PCR, polymerase chain reaction; PNA, peptide nucleic acids.

detected even from three cancer cells using our membrane separation method.

CTC Analysis for Genotyping in a Patient with Lung Cancer

We applied our membrane separation method for genotyping a patient with lung cancer. A 64 year old female patient with stage IV NSCLC harboring an L858R mutation was treated with gefitinib, a first-generation EGFR-TKI. After progression on EGFR-TKI therapy, a re-biopsy was performed from the primary tumor in the left lower lobe. As a T790M point mutation was detected in her tumor, she was treated with osimertinib, a third-generation EGFR-TKI, which is effective against the T790M resistance mutation, as second-line therapy (Figure 5a). After initially responding to osimertinib, her disease progressed after 1.2 years (Figure 5a). CTC analysis revealed no CTCs with a typical phenotype ($DAPI^+$/$EpCAM^+$/$CD45^-$); however, $DAPI^+$/$EpCAM^{-/low}$/$CD45^-$ cells were larger than leukocytes (Figure 5b). Epithelial-to-mesenchymal transition (EMT) is characterized by phenotype changes that include loss of epithelial marker such as EpCAM and gain of mesenchymal marker such as vimentin, and is known to be involved in the acquired resistance to EGFR-TKIs;[23] therefore, we performed additional staining with vimentin as an EMT marker and found that some of these cells were vimentin positive (Figure 5b). Ten cells were collected using a Micro Pick and Place Z robotic system. After whole genome amplification, the amplified DNA was analyzed using the Cobas EGFR Mutation Test v2 (Roche Diagnostics) for detecting EGFR mutations and using the PNA−LNA PCR clamp for detecting the C797S mutation that confers acquired resistance to osimertinib.[24] These genomic analyses revealed that L858R and C797S were detected in the cells, whereas T790M was not (Figure 5a). The emergence of the C797S mutation and loss of T790M are usually associated with osimertinib treatment failure.[25] These results indicate that our method has the potential as an effective alternative tool for genotyping, as well as phenotyping unevaluable cases via cell-free DNA analyses, such as liquid biopsies.

This paper contributes to the development of test kits for clinical trials by identifying the filter specifications and pressure conditions under which practical levels of CTC enrichment can be achieved. Many previous studies have already reported cases of detailed characterization of filtration for separating CTCs[13,17] and of the development of devices that increased the purity of CTCs by methods different from filtration.[5−7] On the other hand, this paper achieved the separation and analysis of CTCs from blood using a simple syringe and filter configuration. This shows the potential of a bedside test kit.

CONCLUSIONS

In this study, we performed oncogene mutation analysis of CTCs using single-cell membrane separation and DNA amplification. By isolating single cancer cells from blood and performing fluorescence assays, we provide a clean and straightforward protocol for enumeration, identification, and subsequent genomic analysis of oncogene mutations in CTCs by microfiltration. We successfully constructed a system to monitor changes in pressure during filtration. This system is expected to provide a tool for evaluating efficient filtration pressure to concentrate CTCs from whole blood. The analysis of the suitability for CTC separation conditions based on the pressure drop of the sample under constant flow drive is a new finding. When filters become clogged, separation performance becomes unstable. In this paper, we succeeded in verifying the pressure conditions under which filter clogging does not occur. Furthermore, the detection of genetic mutations under these conditions indicates that a practical level of enrichment of CTCs has been achieved.

https://doi.org/10.1021/acsmeasuresciau.2c00057
ACS Meas. Sci. Au 2023, 3, 113−119

■ ASSOCIATED CONTENT

Supporting Information

The Supporting Information is available free of charge at https://pubs.acs.org/doi/10.1021/acsmeasuresciau.2c00057.

Evaluation of capture performance for tumor cells in PBS versus those in blood, optical microscope images of microholes, evaluation of pressure drop for PBS and blood samples, and relationship between pressure drop for PBS and syringe speed (PDF)

■ AUTHOR INFORMATION

Corresponding Authors

Daisuke Onoshima − *Institute of Nano-Life-Systems, Institutes of Innovation for Future Society, Nagoya University, Nagoya 464-8601, Japan;* orcid.org/0000-0002-3672-7514; Email: onoshima-d@nanobio.nagoya-u.ac.jp

Tetsunari Hase − *Department of Respiratory Medicine, Nagoya University Graduate School of Medicine, Nagoya 466-8550, Japan;* orcid.org/0000-0002-9653-8424; Email: thase@med.nagoya-u.ac.jp

Authors

Naoto Kihara − *AGC Inc., Tokyo 100-8405, Japan*

Daiki Kuboyama − *Department of Biomolecular Engineering, Graduate School of Engineering, Nagoya University, Nagoya 464-8603, Japan*

Hiromasa Tanaka − *Division of Host Defense Sciences, Department of Integrated Health Sciences, Nagoya University Graduate School of Medicine, Nagoya 461-8673, Japan*

Naoya Ozawa − *Department of Respiratory Medicine, Nagoya University Graduate School of Medicine, Nagoya 466-8550, Japan*

Hiroshi Yukawa − *Institute of Nano-Life-Systems, Institutes of Innovation for Future Society, Nagoya University, Nagoya 464-8601, Japan; Department of Biomolecular Engineering, Graduate School of Engineering, Nagoya University, Nagoya 464-8603, Japan; Center for Low-Temperature Plasma Sciences, Nagoya University, Nagoya 464-8601, Japan;* orcid.org/0000-0002-9352-1520

Mitsuo Sato − *Division of Host Defense Sciences, Department of Integrated Health Sciences, Nagoya University Graduate School of Medicine, Nagoya 461-8673, Japan*

Kenji Ishikawa − *Center for Low-Temperature Plasma Sciences, Nagoya University, Nagoya 464-8601, Japan*

Yoshinori Hasegawa − *Department of Respiratory Medicine, Nagoya University Graduate School of Medicine, Nagoya 466-8550, Japan; National Hospital Organization, Nagoya Medical Center, Nagoya 460-0001, Japan*

Makoto Ishii − *Department of Respiratory Medicine, Nagoya University Graduate School of Medicine, Nagoya 466-8550, Japan*

Masaru Hori − *Center for Low-Temperature Plasma Sciences, Nagoya University, Nagoya 464-8601, Japan*

Yoshinobu Baba − *Institute of Nano-Life-Systems, Institutes of Innovation for Future Society, Nagoya University, Nagoya 464-8601, Japan; Department of Biomolecular Engineering, Graduate School of Engineering, Nagoya University, Nagoya 464-8603, Japan; Institute of Quantum Life Science, Quantum Life and Medical Science Directorate, National Institutes for Quantum Science and Technology (QST), Chiba 263-8555, Japan*

Complete contact information is available at: https://pubs.acs.org/10.1021/acsmeasuresciau.2c00057

Author Contributions

Concept and study design: D.O., T.H., N.K., D.K., and H.T. Data acquisition: N.K., D.K., and N.O. Drafting of the manuscript: D.O., T.H., and D.K. Critical revision of the manuscript for important intellectual content: N.K., H.T., N.O., H.Y., M.S., K.I., Y.H., M.I., M.H., and Y.B. All the authors approved the final version of the manuscript.

Funding

T.H. received personal fees and research funding from AstraZeneca outside the submitted work. Y.H. received personal fees and research funding from AstraZeneca outside the submitted work.

Notes

The authors declare no competing financial interest.

■ ACKNOWLEDGMENTS

This research was supported by the Center of Innovation Program of the Japan Science and Technology Agency. We would like to thank Editage (www.editage.com) for English language editing.

■ REFERENCES

(1) Schweizer, M. T.; Antonarakis, E. S. Liquid biopsy: Clues on Prostate Cancer Drug Resistance. *Sci. Transl. Med.* **2015**, *7*, 312fs45.

(2) Nieva, J. J.; Kuhn, P. Fluid Biopsy for Solid Tumors: A Patient's Companion for Lifelong Characterization of Their Disease. *Future Oncol.* **2012**, *8*, 989−998.

(3) Ozkumur, E.; Shah, A. M.; Ciciliano, J. C.; Emmink, B. L.; Miyamoto, D. T.; Brachtel, E.; Yu, M. Y. P.; Chen, B.; Morgan, J.; Trautwein, A.; Kimura, S.; Sengupta, S. L.; Stott, N. M.; Karabacak, T. A.; Barber, J. R.; Walsh, K.; Smith, P. S.; Spuhler, J. P.; Sullivan, R. J.; Lee, D. T.; Ting, X.; Luo, A. T.; Shaw, A.; Bardia, L. V.; Sequist, D. N.; Louis, S.; Maheswaran, R.; Kapur, D. A.; Haber, M.; Toner, M. Inertial Focusing for Tumor Antigen-Dependent and -Independent Sorting of Rare Circulating Tumor Cells. *Sci. Transl. Med.* **2013**, *5*, 179ra47.

(4) Politi, K.; Ayeni, D.; Lynch, T. The Next Wave of EGFR Tyrosine Kinase Inhibitors Enter the Clinic. *Cancer Cell* **2015**, *27*, 751−753.

(5) West, H. J.; Jin, J. O. Circulating Tumor Cells. *JAMA Oncol.* **2015**, *1*, 394.

(6) Harouaka, R.; Kang, Z.; Zheng, S.; Cao, L. Circulating Tumor Cells: Advances in Isolation and Analysis, and Challenges for Clinical Applications. *Pharmacol. Ther.* **2014**, *141*, 209−221.

(7) Li, Y.-Q.; Chandran, B. K.; Lim, C. T.; Chen, X. Rational Design of Materials Interface for Efficient Capture of Circulating Tumor Cells. *Adv. Sci.* **2015**, *2*, 1500118.

(8) Li, W.; Reátegui, E.; Park, M. H.; Castleberry, S.; Deng, J. Z.; Hsu, B.; Mayner, S.; Jensen, A. E.; Sequist, L. V.; Maheswaran, S.; Haber, D. A.; Toner, M.; Stott, S. L.; Hammond, P. T. Biodegradable Nano-Films for Capture and Non-Invasive Release of Circulating Tumor Cells. *Biomaterials* **2015**, *65*, 93−102.

(9) Diéguez, L.; Winter, M. A.; Pocock, K. J.; Bremmell, K. E.; Thierry, B. Efficient Microfluidic Negative Enrichment of Circulating Tumor Cells in Blood Using Roughened PDMS. *Analyst* **2015**, *140*, 3565−3572.

(10) Cho, W.; Pradhan, R.; Chen, H. Y.; Weng, Y.-H.; Chu, H. Y.; Tseng, F.-G.; Lin, C.-P.; Jiang, J.-K. Rapid Staining of Circulating Tumor Cells in Three-Dimensional Microwell Dialysis (3D-μDialysis) Chip. *Sci. Rep.* **2017**, *7*, 11385.

(11) Kihara, N.; Kuboyama, D.; Onoshima, D.; Ishikawa, K.; Tanaka, H.; Ozawa, N.; Hase, T.; Koguchi, R.; Yukawa, H.; Odaka,

H.; Hasegawa, Y.; Baba, Y.; Hori, M. Low-Autofluorescence Fluoropolymer Membrane Filters for Cell Filtration. *Jpn. J. Appl. Phys.* **2018**, *57*, 06JF03.
(12) Ilie, M.; Hofman, V.; Long-Mira, E.; Selva, E.; Vignaud, J.-M.; Padovani, B.; Mouroux, J.; Marquette, C.-H.; Hofman, P. "Sentinel" circulating tumor cells allow early diagnosis of lung cancer in patients with chronic obstructive pulmonary disease. *PLoS One* **2014**, *9*, No. e111597.
(13) Tang, Y.; Shi, J.; Li, S.; Wang, L.; Cayre, Y. E.; Chen, Y. Microfluidic Device with Integrated Microfilter of Conical-Shaped Holes for High Efficiency and High Purity Capture of Circulating Tumor Cells. *Sci. Rep.* **2014**, *4*, 6052.
(14) Adams, D. L.; Zhu, P.; Makarova, O. V.; Martin, S. S.; Charpentier, M.; Chumsri, S.; Li, S.; Amstutz, P.; Tang, C.-M. The Systematic Study of Circulating Tumor Cell Isolation Using Lithographic Microfilters. *RSC Adv.* **2014**, *9*, 4334−4342.
(15) Adams, D. L.; Stefansson, S.; Haudenschild, C.; Martin, S. S.; Charpentier, M.; Chumsri, S.; Cristofanilli, M.; Tang, C.-M.; Alpaugh, R. K. Cytometric Characterization of Circulating Tumor Cells Captured by Microfiltration and Their Correlation to the CellSearch(®) CTC Test. *Cytometry, Part A* **2015**, *87*, 137−144.
(16) Livak-Dahl, E.; Sinn, I.; Burns, M. Microfluidic Chemical Analysis Systems. *Annu. Rev. Chem. Biomol. Eng.* **2011**, *2*, 325−353.
(17) Coumans, F. A.; van Dalum, G.; Beck, M.; Terstappen, L. W. Filtration Parameters Influencing Circulating Tumor Cell Enrichment from Whole Blood. *PLoS One* **2013**, *8*, No. e61774.
(18) Cross, S. E.; Jin, Y.-S.; Rao, J.; Gimzewski, J. K. Nanomechanical Analysis of Cells from Cancer Patients. *Nat. Nanotechnol.* **2007**, *2*, 780−783.
(19) Meng, S.; Tripathy, D.; Frenkel, E. P.; Shete, S.; Naftalis, E. Z.; Huth, J. F.; Beitsch, P. D.; Leitch, M.; Hoover, S.; Euhus, D.; Haley, B.; Morrison, L.; Fleming, T. P.; Herlyn, D.; Terstappen, L. W. M. M.; Fehm, T.; Tucker, T. F.; Lane, N.; Wang, J.; Uhr, J. W. Circulating Tumor Cells in Patients with Breast Cancer Dormancy. *Clin. Cancer Res.* **2004**, *10*, 8152−8162.
(20) Sequist, L. V.; Bell, D. W.; Lynch, T. J.; Haber, D. A. Molecular Predictors of Response to Epidermal Growth Factor Receptor Antagonists in Non-Small-Cell Lung Cancer. *J. Clin. Oncol.* **2007**, *25*, 587−595.
(21) Lynch, T. J.; Bell, D. W.; Sordella, R.; Gurubhagavatula, S.; Okimoto, R. A.; Brannigan, B. W.; Harris, P. L.; Haserlat, S. M.; Supko, J. G.; Haluska, F. G.; Louis, D. N.; Christiani, D. C.; Settleman, J.; Haber, D. A. Activating Mutations in the Epidermal Growth Factor Receptor Underlying Responsiveness of Non-Small-Cell Lung Cancer to Gefitinib. *N. Engl. J. Med.* **2004**, *350*, 2129−2139.
(22) Kobayashi, S.; Boggon, T. J.; Dayaram, T.; Jänne, P. A.; Kocher, O.; Meyerson, M.; Johnson, B. E.; Eck, M. J.; Tenen, D. G.; Halmos, B. EGFR Mutation and Resistance of Non−Small-Cell Lung Cancer to Gefitinib. *N. Engl. J. Med.* **2005**, *352*, 786−792.
(23) McGowan, M.; Kleinberg, L.; Halvorsen, A. R.; Helland, Å.; Brustugun, O. T. NSCLC Depend upon YAP Expression and Nuclear Localization After Acquiring Resistance to EGFR Inhibitors. *Genes Cancer* **2017**, *8*, 497−504.
(24) Thress, K. S.; Paweletz, C. P.; Felip, E.; Cho, B. C.; Stetson, D.; Dougherty, B.; Lai, Z.; Markovets, A.; Vivancos, A.; Kuang, Y.; Ercan, D.; Matthews, S. E.; Cantarini, M.; Barrett, J. C.; Jänne, P. A.; Oxnard, G. R. Acquired EGFR C797S Mutation Mediates Resistance to AZD9291 in Non-Small Cell Lung Cancer Harboring EGFR T790M. *Nat. Med.* **2015**, *21*, 560−562.
(25) Leonetti, A.; Sharma, S.; Minari, R.; Perego, P.; Giovannetti, E.; Tiseo, M. Resistance Mechanisms to Osimertinib in EGFR-Mutated Non-Small Cell Lung Cancer. *Br. J. Cancer* **2019**, *121*, 725−737.

https://doi.org/10.1021/acsmeasuresciau.2c00057
ACS Meas. Sci. Au 2023, 3, 113−119